

Physics in plasmonic and Mie scattered near-field for efficient surface-enhanced Raman scattering template

Akira Zenidaka · Toshiyuki Honda ·
Mitsuhiro Terakawa

Received: 27 April 2011 / Accepted: 13 July 2011 / Published online: 26 August 2011
© Springer-Verlag 2011

Abstract We describe the physics of the SERS based on the optical near-field intensity enhancement on the metallic (plasmonic) and the nonmetallic (Mie scattering) nanostructured substrates with two-dimensional (2D) periodic nanohole arrays. The calculation by the Finite-Difference Time-Domain (FDTD) method revealed that the optical intensity enhancement increases with the increase of the thickness of a gold film coating on the nonmetallic (dielectric) nanostructured Si, GaAs, and SiC substrates. The resonance spectrum shifts with the changes in the geometrical structure of the void diameter and inter-void distance. It was clarified that the optical intensity enhancement obtained with the gold-coated substrate is equivalent to that with a gold substrate at 70-nm thick gold coating on the dielectric substrates in this structure. The resonance spectral bandwidth for Mie scattering and plasmonic near-fields is different. Therefore, if the Stokes line of the Raman scattering is located within the resonance bandwidth, the SERS signal is enhanced proportionally to the fourth power of the electric near-field. However, if the Stokes shift is located out of the resonance bandwidth, the SERS signal enhancement is only proportional to the square of the scattered near-field.

1 Introduction

The use of enhanced optical near-field on a nanostructured substrate surface has attracted much attention for the development of smart optical, electro-optical, and biological devices. Surface-enhanced Raman scattering (SERS) is a

Raman spectroscopic technique which employs the phenomenon that Raman scattering of molecules is drastically enhanced by the enhanced optical near-field on the surface of nanostructures [1, 2]. SERS technique enables to detect an ultra-low concentration of analyte molecules adsorbed on the surface even with low-intensity laser excitation. Many papers on the SERS have been published, which describe the highly efficient Raman scattering enhancement using metallic substrates. Metallic and metal-coated nanostructures of periodic nanohole arrays (voids) are typical templates for SERS which show highly enhanced optical intensity on the surface [3–9]. It is noted that the nanostructure of periodic nanohole arrays has several advantages to be used for SERS template. It is easily fabricated by reactive ion etching (RIE) [6], electron-beam lithography (EBL) [7], focused ion beam (FIB) [8], and nanosphere lithography (NSL) [9]. In addition, the measurement can be performed efficiently by matching the void size to the size of an analyte molecule. We have recently reported that the nanostructure of periodic spherical nanohole arrays shows not only the high peak optical intensity, but also higher spatially averaged optical intensity enhancement [10]. This fact means that the highly enhanced near-field zone distributes densely on the substrate.

Bare nonmetallic nanostructures such as porous silicon film [11], crystalline TiO₂ substrate [12], Zn-doped TiO₂ nanoparticles [13], and GaP nanoparticles [14] have also been investigated for the enhancement of the Raman scattering. The near-field enhancement of Raman scattering signals was obtainable with randomly grown high-dielectric-permittivity ZnO nanorods [15]. The Raman scattering enhancement by using nonmetallic nanostructures can be considered to originate from the Mie scattering near-field. Although the nonmetallic SERS templates have an advantage in their simple fabrication processes, the properties of nonmetallic SERS templates are not fully understood

A. Zenidaka · T. Honda · M. Terakawa (✉)
School of Integrated Design Engineering, Keio University,
3-14-1, Hiyoshi, Kohoku-ku, Yokohama-shi 223-8522, Japan
e-mail: terakawa@elec.keio.ac.jp

compared to the metallic SERS templates which have been widely investigated. Detailed investigation on the physics governing the enhanced optical field generation process of the metallic (plasmonic) and the nonmetallic (resonant Mie scattering) will be necessary for the efficient SERS template providing high optical intensity enhancement with a simple fabrication process. Of course, smart previous work on the dielectric *spheres* with metal thin film coating has been published by Prof. N. Halas group at Rice University [16]. They have investigated mainly the scattering cross section and plasmon resonance spectrum.

In this paper, we describe the underlying physics of the optical intensity enhancement on the metallic and the non-metallic substrate surface with periodic nanohole arrays. The electric field enhancement on a silicon (Si) substrate was investigated with and without the gold film coating on the substrate surface. The dependence of the optical intensity enhancement on the thickness of the gold film coating was also investigated to understand the SERS properties by comparing the plasmonic and the Mie scattering near-field SERS templates. The enhancements on the surface of a gallium arsenide (GaAs) and silicon carbide (SiC) substrates were also investigated and their properties were compared with that of Si substrate. From the viewpoint of practical use, GaAs and SiC are the promising alternatives for Si as a nonmetallic (semiconductor) substrate. The difference in resonance spectra and spectral bandwidth of the metallic and the nonmetallic substrates and its optical intensity enhancement physics will be discussed in detail.

2 Simulation system and procedure

The electromagnetic field enhancement distribution on the nanostructured surface is calculated by the three-dimensional (3D) Finite-Difference Time-Domain (FDTD) method [17]. Figure 1 shows the 3D view (a), the cross-sectional view (b), and the top view (c) of the simulation system. The numerical simulation is carried out for the 3D system. Arrays of hemispherical holes (voids) on a substrate are defined as the nanostructure for the SERS template. Two-dimensional (2D) arrays of seven holes are set in the area for the simulation system. This type of structures can simply be fabricated by nano imprint process [18]. To simulate the infinite arrays of holes, periodic boundary conditions are applied for the xz and yz plane (the x , y , z axes are defined as shown in Fig. 1). The height (z axis) of the calculation area is set to 1300 nm and the light source is set upside the calculation area 750 nm distant from the substrate surface. The absorbing boundary condition is applied on the xy plane. The optical intensity enhancement on a Si substrate was investigated with and without a gold film coating. In this paper the enhancement was evaluated by the

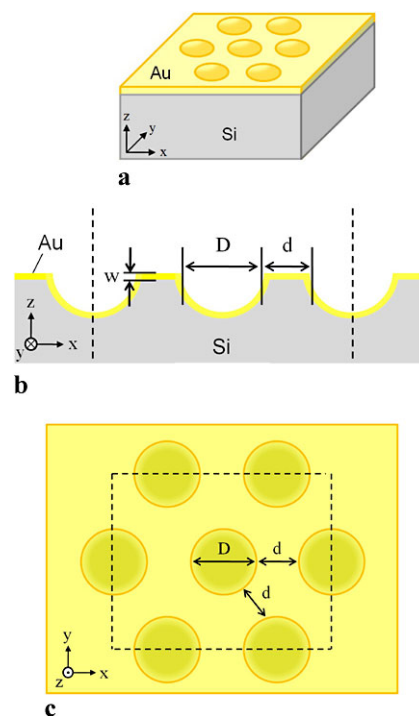


Fig. 1 Schematic of the simulation system. 3D view (a), top view (b), and cross-sectional view (c) of the system. 2D arrays of seven holes are set in the calculation area for all simulation systems. Periodic boundary conditions are applied on the xz and yz plane. The area shown in dashed lines indicates the calculation area. The light source is placed upside the calculation area, 750 nm distant from the gold substrate

square of the optical field strength, not by the fourth power of the electric field which commonly used for the evaluation of a plasmonic SERS template [19, 20]. The reason for the evaluation by the square of the electric field is due to the bandwidth of the resonance spectrum. The dependence of the electric field enhancement on the void diameter D was investigated from $D = 300$ to 500 nm. The inter-void distance d is defined as the distance between the edges of the voids. In the simulation system, D and d are the parameters including the thickness w of the gold film coating, in which D and d can be constant for different thicknesses of the gold film coating with the same geometrical surface structure. In all simulations, a circularly polarized incident wave was used. Electric field strength of the incident wave is set to 1 V/m. The optical intensity enhancement on GaAs and SiC substrates is also investigated.

3 Results and discussion

Figure 2 shows the enhanced optical intensity distributions and intensity profiles on the surface of gold-coated Si substrate. The void diameter D and the inter-void distance d were set to 300 and 200 nm, respectively. The thickness of the gold film is set to 50 nm in Figs. 2(a) and 2(b). The

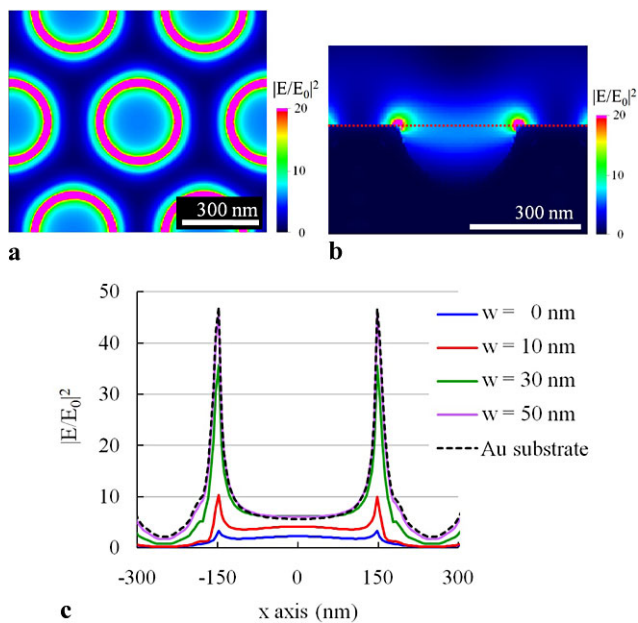


Fig. 2 Enhanced optical intensity distributions (**a**, **b**) and intensity profiles (**c**) on the surface of gold-coated Si substrate. The wavelengths of the incident wave are set to 532 nm. (**a**) Top view of the enhanced optical intensity distribution on xy plane. (**b**) Cross-sectional view of the enhanced optical intensity distribution on the xz plane. The void diameter D and the inter-void distance d were set at 300 and 200 nm, respectively

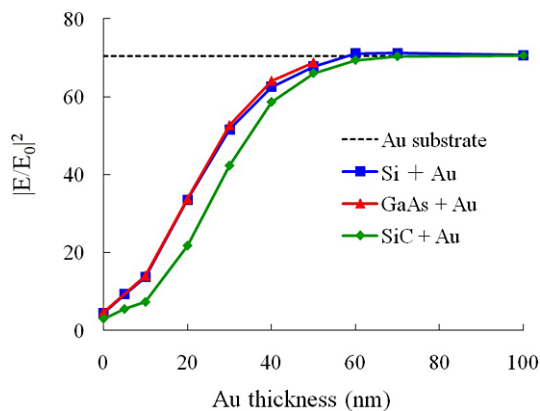


Fig. 3 Dependence of the peak optical intensity enhancement at 532 nm on the thickness of the gold film coating on Si, GaAs, and SiC substrates. The peak optical intensity enhancement obtained with a gold template of the same nanostructure is also shown in the figure. The thickness $w = 0$ indicates bare dielectric substrates. The void diameter D and the inter-void distance d were set to 300 and 200 nm, respectively

high optical intensity localization so-called hotspot appears on the edges of the hemispherical voids with the excitation wavelength of 532 nm.

Figure 3 shows the dependence of the peak optical intensity enhancement at 532 nm on the thickness of the gold film coating on the Si, GaAs, and SiC substrates. The incident wavelength, void diameter D , and the inter-void distance d

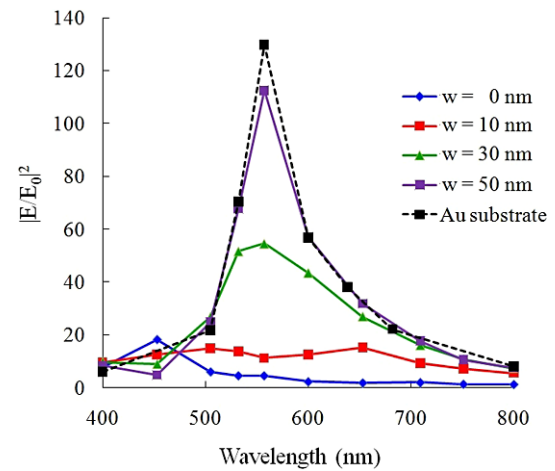


Fig. 4 Dependence of the peak optical intensity enhancement on the pumping wavelength for Si substrate coated with different thicknesses of gold film. The peak optical intensity enhancement obtained by a gold template of the same geometrical structure is also shown in the figure. The void diameter D and the inter-void distance d were set at 300 and 200 nm, respectively

are set to 532, 300, and 200 nm, respectively. The refractive indices of Si, GaAs, and SiC at 532 nm are 4.14, 4.12, and 2.67, respectively [21]. The parameters D and d were found to be the optimum pair for the optical intensity enhancement with a gold template at the excitation wavelength of 532 nm [10]. Note that the void diameter and inter-void distance are kept constant. The resonant Mie scattering occurs at 450 nm approximately, as shown in Fig. 4. The optical intensity enhancement was investigated for Si, GaAs, and SiC substrates. The bare dielectric substrates show optical intensity enhancements lower than 10 for the three substrates. The optical intensity increases with the increase of the thickness of the gold coating and approaches asymptotically to the intensity enhancement obtained with the bare gold substrate. The optical intensities obtained with Si and GaAs are found to be higher than that obtained with SiC at the gold coating thicknesses less than 50–60 nm. It is because the refractive indices of the Si and GaAs are higher than that of SiC. With the gold coating is thicker than 70 nm, the optical intensity enhancement for all substrates is equivalent to that obtained with the gold nanostructured substrate. The optical penetration depth of gold at 532 nm is shorter than 70 nm, and therefore, the incident 532 nm beam cannot see the dielectric substrate but can see only the gold layer. With no gold coating, the enhanced near-field by the resonant Mie scattering may work, and between the two sides the incident wave can see plasmonic process mediated with high-dielectric substrate.

The dependence of the optical intensity enhancement on the excitation wavelength is shown in Fig. 4. The void diameter D and the inter-void distance d were set to 300 and 200 nm, respectively. The calculation was performed for the

thickness $w = 0$ (bare Si substrate) and the gold film thicknesses of 10, 30, and 50 nm on Si substrate. The optical intensity achieved with a gold substrate is also shown in the figure. The bare Si substrate shows a peak optical intensity enhancement at the resonant Mie scattering wavelength at 450 nm approximately, while the Si substrates coated with 30- and 50-nm thick gold film show peak optical intensities at a wavelength around 550 nm, at which the nanostructured gold substrate gives a highest enhancement factor. The results stem from the optical penetration depth in the gold film and the peak enhancement factor shifts from the resonant Mie scattering spectrum to the plasmon resonance spectrum. To get large plasmon resonance SERS, the gold film coating is thicker than 50–60 nm in this geometry. We previously investigated the enhanced Raman scattering properties of bare ZnO nanorods [15]. In the previous study, we investigated the dependence of the size parameter in the Mie scattering theory on the near-field enhanced Raman scattering properties. The experimental result was explained theoretically by the size parameter described in the Mie scattering theory, not by surface plasmon polaritons [15]. SERS templates using a bare nonmetallic substrate have a potential to achieve the simplification and the cost reduction in nanofabrication process.

Figure 5(a) shows the dependence of the optical intensity enhancement on the excitation wavelength for a bare nanostructured Si substrate. The optical intensity was investigated for three different values of D at a constant value of $d = 200$ nm. The peak optical intensity is highest with $D = 300$ nm. The Mie resonance scattering wavelength shows the red shift with the increase of D . The red shift in wavelength corresponds to the increase in the value of $D + d$. Figure 5(b) shows the dependence of the optical intensity enhancement on the excitation wavelength for the Si substrate with a 50-nm thick gold film coating with different values of D . With this thickness, the resonant spectrum corresponds to the plasmon resonant spectrum obtained with the gold substrate. The resonance wavelengths obtained with gold-coated substrates are longer than those with bare Si nanostructured substrates under the same geometrical structure conditions. As a result, the plasmonic enhancement factor is about 10 times larger than the Mie scattering near-field in this geometry. Figure 5(c) shows the dependence of the optical intensity enhancement on the excitation wavelength for the gold-coated substrate with different values of d at a constant value of $D = 300$ nm. The plasmon polaritons are coupled each other and if the inter-void distance changes the field enhancement factor changes. With the 300-nm diameter voids, the inter-void distance of 300 nm gives a highest enhancement factor of over than 250. The shift of the peak resonance wavelength stems from the grating effect.

Figure 6 shows the normalized resonance spectral bandwidth for the gold and Si nanostructured substrates. The

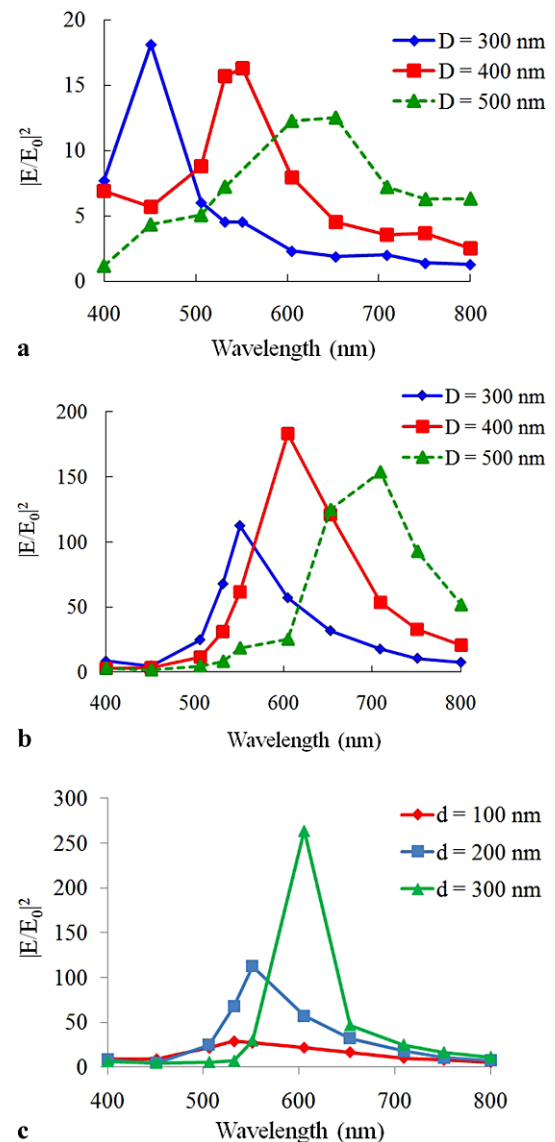


Fig. 5 Dependence of the peak optical intensity enhancement on the excitation wavelength for the different geometrical parameters: (a) bare Si substrate at $D = 300, 400,$ and 500 nm at $d = 200$ nm constant, (b) Si substrate coated with a 50-nm thick gold film at $D = 300, 400,$ and 500 nm at $d = 200$ nm constant, (c) Si substrate coated with a 50-nm thick gold film at $d = 100, 200,$ and 300 nm at $D = 300$ nm constant

void diameter D and the inter-void distance d are for both substrates set to 300 and 200 nm, respectively. While the Si nanostructured substrate has the narrow resonance bandwidth (FWHM) of 18 nm centered at 450 nm, the gold substrate has the wide bandwidth (FWHM) of 83 nm centered at 550 nm. This means that the Q factor for the plasmon resonance of gold is as small as 7.0 approximately. In other words, gold is lossy in the visible region of the spectrum. However, silicon has a Mie scattering resonance bandwidth much narrower than the gold plasmon resonance. The enhancement factor of Raman scattering signal (Stokes line)

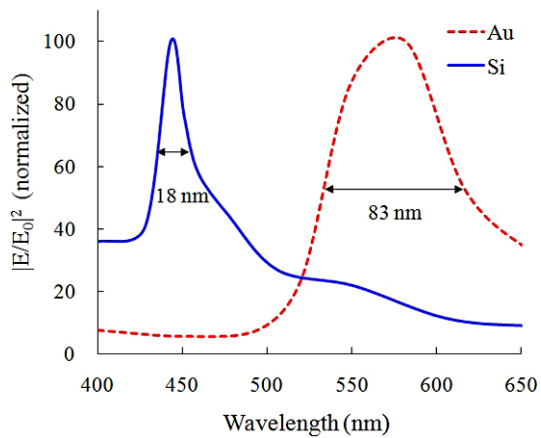


Fig. 6 The normalized resonance spectral bands for gold and Si substrates with the same geometrical structures. The void diameter D and the inter-void distance d were set to 300 and 200 nm, respectively. Note that the bandwidths are different for both cases

is mainly dependent on the near-field enhancement factor and resonance bandwidth. Of course, the chemical effect of the Raman molecule adsorbed on the nanostructured surface may work. One of the typical Raman Stokes shifts observed for Rhodamine 6G (R6G) is 1364 cm^{-1} [22], which corresponds to the Stokes shift of 29.4 and 41.6 nm in spectrum at the excitation wavelength of 450 and 532 nm, respectively. More favorably the excitation wavelength should be tuned to the respective resonance center wavelengths, as shown in Fig. 6, to get strong Stokes line intensity. If the R6G is optically pumped at 450 nm, the Raman Stokes line is *not* located within the resonance spectral bandwidth in the case of the bare Si nanostructured substrate due to the narrow resonance bandwidth. In this case, the Mie scattered near-field SERS is increased only by the enhanced near-field, corresponding to the fact that the SERS signal enhancement is only proportional to the square of the near-field. If the Stokes shift is much smaller than the resonance bandwidth, the SERS signal enhancement may be proportional to the fourth of the near-field even in the resonance Mie scattering regime. Conversely, the gold substrate and gold-coated substrate have a wide resonance bandwidth, in which the many Raman Stokes lines may be located. Hence, the Stokes line may additionally be amplified by the enhanced near-field via mode coupling process, resulting in that the total enhancement of the SERS signal is proportional to the fourth power of the electric field. If pumped at 532 nm, the Stokes shift of R6G is 41.6 nm (Stokes line is 573.6 nm), the total enhancement of the SERS signal is actually proportional to the fourth power of the electric field. However, if the Stokes shift is large enough for relatively small molecules and the Stokes line is located out of the resonance bandwidth, the SERS signal enhancement may be only proportional to the square of the near-field even in the plasmonic SERS template.

4 Conclusions

We have studied the optical near-field intensity enhancement on the gold-coated Si, GaAs, and SiC substrates with periodic nanohole arrays. With the increase of the thickness of the gold coating, the optical intensity enhancement increases and approaches asymptotically to the intensity obtained with a gold nanostructured substrate. In addition the red shift of the resonance spectrum was observed. It was clarified that the optical intensity enhancement obtained with the gold-coated substrate is equivalent to that with a gold substrate at 70-nm thick gold coating on the dielectric substrates in this structure. The resonance spectral bandwidth for Mie scattering and plasmon polaritons near-fields is different. Therefore, if the Stokes line of the SERS is located within the bandwidth, the SERS signal is proportional to the fourth power of the electric field. However, if the Stokes shift is located out of the resonance bandwidth, the SERS signal enhancement may be only proportional to the square of the near-field in both Mie scattered near-field and plasmonic scattered near-field.

Acknowledgements This work was supported by a Grant-In-Aid for Scientific Research B (23360161) from the Ministry of Education, Culture, Sport, Science, and Technology of Japan and a grant from the Amada Foundation for Metal Work Technology (AF-2010209).

References

1. A. Campion, P. Kambhampati, *Chem. Soc. Rev.* **27**, 241 (1998)
2. K.A. Willets, R.P. Van Duyne, *Annu. Rev. Phys. Chem.* **58**, 267 (2007)
3. R.M. Cole, J.J. Baumberg, F.J. Garcia de Abajo, S. Mahajan, M. Abdelsalam, P.N. Bartlett, *Nano Lett.* **7**, 2094 (2007)
4. S. Mahajan, R.M. Cole, B.F. Soares, S.H. Pelfrey, A.E. Russell, J.J. Baumberg, P.N. Bartlett, *J. Phys. Chem. C* **113**, 9284 (2009)
5. Q. Yu, P. Guan, D. Qin, G. Golden, P.M. Wallace, *Nano Lett.* **8**, 1923 (2008)
6. S.H. Lee, K.C. Bantz, N.C. Lindquist, S. Oh, C.L. Haynes, *Langmuir* **25**, 13685 (2009)
7. J.T. Bahns, Q. Guo, J.M. Montgomery, S.K. Gray, H.M. Jaeger, L. Chen, *J. Phys. Chem. C, Nanomater. Interfaces* **113**, 11190 (2009)
8. J.R. Anema, A.G. Brolo, P. Marthandam, R. Gordon, *J. Phys. Chem. C* **112**, 17051 (2008)
9. J. Masson, M. Murray-Méthot, L.S. Live, *Analyst* **135**, 1483 (2010)
10. A. Zenidaka, Y. Tanaka, T. Miyanishi, M. Terakawa, M. Obara, *Appl. Phys. A* **103**, 225 (2011)
11. S.K. Deb, N. Mathur, A.P. Roy, S. Banerjee, A. Sardesai, *Solid State Commun.* **101**, 283 (1997)
12. H. Yamada, Y. Yamamoto, *Surf. Sci.* **134**, 71 (1983)
13. L. Yang, Y. Zhang, W. Ruan, B. Zhao, W. Xu, J.R. Lombardi, *J. Raman Spectrosc.* **41**, 721 (2010)
14. S. Hayashi, R. Koh, Y. Ichiyama, K. Yamamoto, *Phys. Rev. Lett.* **60**, 1085 (1988)
15. M. Terakawa, Y. Tanaka, G. Obara, T. Sakano, M. Obara, *Appl. Phys. A* **102**, 661 (2011)
16. S. Lal, N.K. Grady, J. Kundu, C.S. Levin, J.B. Lassiter, N.J. Halas, *Chem. Soc. Rev.* **37**, 898 (2008)

17. A. Taflove, S.C. Hagness, *Computational Electrodynamics: The Finite-Difference Time-Domain Method*, 2nd edn. (Artech House, Boston, 2000)
18. Z. Yu, H. Gao, W. Wu, H. Ge, S.Y. Chou, *J. Vac. Sci. Technol. B* **21**, 2874 (2003)
19. M. Inoue, K. Ohtaka, *J. Phys. Soc. Jpn.* **52**, 3853 (1983)
20. T. Itoh, K. Yoshida, V. Biju, Y. Kikkawa, M. Ishikawa, Y. Ozaki, *Phys. Rev. B* **76**, 085405 (2007)
21. D.D. Palik (ed.), *Handbook of Optical Constants of Solids* (Academic Press, San Diego, 1998)
22. W. Li, X. Li, N. Yu, *Chem. Phys. Lett.* **312**, 28 (1999)